DISCLAIMER

This report was prepared as an account of work sponsored by an agency of the United States Government. Neither the United States Government nor any agency thereof, nor any of their employees, makes any warranty, express or implied, or assumes any legal liability or responsibility for the accuracy, completeness, or usefulness of any information, apparatus, product, or process disclosed, or represents that its use would not infringe privately owned rights. Reference herein to any specific commercial product, process, or service by trade name, trademark, manufacturer, or otherwise does not necessarily constitute or imply its endorsement, recommendation, or favoring by the United States Government or any agency thereof. The views and opinions of authors expressed herein do not necessarily state or reflect those of the United States Government or any agency thereof. Reference herein to any social initiative (including but not limited to Diversity, Equity, and Inclusion (DEI); Community Benefits Plans (CBP); Justice 40; etc.) is made by the Author independent of any current requirement by the United States Government and does not constitute or imply endorsement, recommendation, or support by the United States Government or any agency thereof.

ANL/NSE-25/30

Benchmark Exercise Report for Experimental Study of Bubble Scrubbing in Sodium Pool

Nuclear Science and Engineering Division

About Argonne National Laboratory

Argonne is a U.S. Department of Energy laboratory managed by UChicago Argonne, LLC under contract DE-AC02-06CH11357. The Laboratory's main facility is outside Chicago, at 9700 South Cass Avenue, Argonne, Illinois 60439. For information about Argonne and its pioneering science and technology programs, see www.anl.gov.

ANL/NSE-25/30

Benchmark Exercise Report for Experimental Study of Bubble Scrubbing in Sodium Pool

Dong Hoon Kam, David Grabaskas
Nuclear Science and Engineering Division
Argonne National Laboratory

Kyle Becker, Mark Anderson
Department of Mechanical Engineering
University of Wisconsin-Madison

Jun 17, 2025

Abstract

Mechanistic source term (MST) analyses are likely to be an important part of advanced reactor licensing applications. For the purpose, an MST analysis code applicable to newly introduced advanced reactors, called SRT (Simplified Radionuclide Transport) code, has been developed by Argonne National Laboratory. SRT can track overall behaviors of radionuclides especially in metal fuel-based sodium fast reactors (SFRs) and microreactors. Throughout the simulation, migration inside fuel pins before failure, interaction with coolant (for SFR), removal/leakage in cover gas and containment (or confinement), and environmental dose impacts are considered alongside radioactive decay for short-lived nuclides. Among the postulated process, pool scrubbing phenomenon, especially under sodium pool condition, has been identified as high importance with limited supportive data. The phenomenon plays a crucial role in assessing the degree of radiological impacts as radioactive aerosols or vapors are efficiently and effectively removed during the process.

To provide validation basis for SRT in assessing pool scrubbing performance inside sodium pools, the University of Wisconsin-Madison performed tests including extensive parametric effects. Separate effect tests were conducted to directly evaluate the SRT models and to estimate degree of contribution by each contributing factor. Specifically, bubble size, aerosol size, aerosol density, aerosol concentration, pool depth, system temperature, and bubble swarm effects were considered. According to the parametric effects, decontamination performance enhances with decreasing bubble size, large density, and deeper pool height. Aerosol concentration provides no effect for the whole range of interest, and pool temperature variation shows minor effects under the considered temperature condition. When multiple bubbles are injected generating a bubble swarm condition, DF performance further enhances by bubble interactions and turbulence characteristics. The measurement shows the exceptional importance of aerosol size range considered, with the lowest decontamination, where most radionuclides are expected to escape.

Table Of Contents

Figures

Tables

1 Introduction

Recently, the U.S. Nuclear Regulatory Commission (NRC) has emphasized the importance of mechanistic approaches for source term analysis, enabling the realistic evaluation of the transport and retention of radioactive material [1, 2]. The practical and realistic approach is expected to provide increased flexibility to reactor vendors. However, the unique phenomena associated with advanced reactor MST analyses may require new modeling tools and verification data.

Under the high demands, a code for mechanistic source term analysis has been developed by Argonne National Laboratory (Argonne), called Simplified Radionuclide Transport (SRT) code. SRT describes overall behaviors of radioactive elements before and after the breach of fuel pins. Status inside the cladding is determined including migration, followed by successive simulations on the radionuclide behaviors along the trajectory inside vessel, within containment (or confinement), and finally toward the environment. Based upon the amount released, dose impact to the surroundings is also calculated. Throughout the process, radioactive nuclides are removed, leaked, and decay. SRT can be applied to sodium fast reactors (SFRs) and microreactors with metal fuels.

After fuel pin failure, radionuclides are ejected into the primary sodium system. This includes the potential creation of radionuclide aerosols within noble gas bubbles in the sodium pool. Fortunately, ejected aerosols may be removed by "pool scrubbing." Some fraction of the released aerosols may escape from the pool system, not perfectly being scrubbed during bubble rise. A fraction of the amount released over the escaped is defined as a decontamination factor (DF), representing degree of pool scrubbing performance. According to thorough assessment by Grabaskas et al. [3], the phenomenon was identified as a major contributor to the expected uncertainty during quantifying the amount released toward environments.

During bubble rise, multiple mechanisms take part in the removal process. As a mechanistic and representative approach, Fuchs [4] has included major phenomena such as Brownian diffusion, inertial impaction, gravitational sedimentation, and vapor condensation. Brownian diffusion plays a dominant role on the decontamination process especially for small-sized aerosols, while both inertial impaction and gravitational sedimentation majorly affects for large aerosols. Preceding simulation approaches mainly focused on conventional large water reactors [5-13], simulating pool scrubbing phenomenon in suppression chamber or safety facilities like containment venting system. Among them, Owczarski and Burk [6] developed a pool scrubbing basis for the MELCOR, an integrated code to simulate accident progression in nuclear power plants, and Ramsdale et al. [8] summarized a pool scrubbing code, called BUSCA, with mechanistic approaches. In parallel, several measurements have also been performed to assess parametric effects and to provide validation basis [14-30]. For example, Kaneko et al. [14] assessed a wide range of parameters including injected gas properties, aerosol size and density, pool depth, and nozzle diameter. Other following studies included some or similar parameters and showed expected tendencies. In addition, Diao et al. [23] further assessed the jet geometry with orientation to reflect high pressure-induced jet ejection with radioactive nuclides inside. According to their measurement, the injection gas pressure had crucial effects on the overall decontamination performance, and the pressure of 0.3 MPa was onset criterion for critical flow in their geometry, beyond which the scrubbing efficiency reached up to nearly perfect removal.

Still, approaches that can be directly applied to advanced reactors have been quite limited up to recently. Miyahara et al. [31] measured iodine gas removal performance inside sodium pool, considering the oxide fuel design adopted in Japan. In their test, an iodine and xenon gas mixture was prepared inside a quartz ball, and the ball was cracked to inject bubble into the sodium system. Various conditions including bubble size, pool height, and system temperature were considered, and bubble rise velocity was measured through void sensors. As a preliminary approach, the bubble size was determined based on the amount of gas mixture initially supplied, postulating possible gap from the realistic dimension. Test condition covered relatively high temperature environments, which is expected to include both normal and abnormal situations in SFRs. Independently, Miyahara and Sagawa [32] performed analytical analysis describing experiments by Miyahara et al. [31]. Diffusion and convection phenomena were considered for the iodine gas removal process inside spherical bubble. Kam et al. [33] tracked iodine gas removal performance in a sodium pool based on Ramsdale et al. [8]'s mechanistic approach for spherical cap bubbles. The approach was validated based on information prepared from Miyahara et al. [31], where relatively large bubble size was provided in accordance with the initial gas mixture volume. Pradeep and Sharma [34] developed a mechanistic analysis approach based on Fuchs [4] to simulate decontamination performance of radioactive aerosols as for water reactors, targeting for sodium reactors.

Previous measurements had some limitations to thoroughly validate mechanistic approaches. For example, independent bubble condition is generally assumed for analytical calculation, while measurement for such independent geometry with aerosol inclusion was insufficient. In trying to assess each parameter's individual effect, Becker and Anderson [26] measured DF under water condition as an initial approach, considering various parametric variation. A single bubble and bubble swarm were realized with aerosols inside, and bubble size, aerosol size, aerosol density (aluminum and nickel powders), aerosol concentration, and pool depth effects were evaluated providing independent contribution of each. The study mainly focused on providing validation basis for bubble scrubbing module in SRT developed by Argonne, by which the consisting parameters can be independently validated. Based on the provided information and uncertainty values for each parameter, Kam et al. [13] performed validation work for bubble size and swarm effects. In their study, DF distribution was considered with the uncertainty, and mean of those distribution has been introduced, compared with DF values acquired by mean values of parameters. Later, Becker and Anderson [35] further included sodium pool for practical purpose. In the latter experiment, an additional material, tungsten, was included in the test matrix to account for heavy radionuclides during the fuel pin failure, and temperature condition was varied.

The prime objective of this report is summarizing results with overall tendencies from the benchmark experiment for sodium pool. Throughout the following sections, parametric effects are assessed, and each of parameter's independent contribution has been evaluated. By measuring DF values for each single bubble, mechanistic approaches adopted in SRT can be directly validated, which further enables verified prediction and uncertainty analysis. The considered parameters are bubble size, aerosol size, aerosol density, aerosol concentration, pool height, system temperature, and bubble swarm condition.

2 Experimental Conditions

2.1 Aerosols and Apparatus

Surrogate materials for radioactive nuclides are used as aerosol particles: aluminum (mean weight diameter of 0.5 um), nickel (mean weight diameter of 0.18 um), and tungsten powders (mean weight diameter of 0.1 um). Tungsten, with relatively high density, is further considered to account for heavy elements such as actinides. Through the aerosol generator (SAG 410/U Solid Aerosol Generator by TOPAS) and a venturi, each type of aerosols has been supplied. SAG 410 uses a rotating ring to supply the target powders with constant and reproducible amounts and is operated by continuous flow, and thus, an additional dilution flow is required to achieve high concentration of aerosols. For single bubble tests, an inverted nozzle has been adopted to ensure relatively large bubbles with minimized breakups. The dimension of the nozzle is 2.54 cm in diameter, and 1.27 cm in height. Two types of inverted funnel shapes are considered on the nozzle structure to include wide range of bubble sizes. Each has base diameter of 1.47 and 1.91 cm, respectively, with 30^{o} angle.

The test array consists of test column, pressure tank, and collection system in large (Figure 1). The test column is composed of an 8-inch, schedule 10, 316 stainless steel pipe with 87 L of sodium inside. Dimension of the test column has been designed to have negligible impact on bubble dynamics. Temperature of the pool is traced by 5 thermocouples (1/8-inch, ungrounded K-type thermocouples with $\pm$ 2.2 ^{o}C uncertainty) inserted along the height of the structure, and the insertion depth is set to be 1 cm to avoid disruption on bubble paths. The pool temperature is maintained with tape-type heaters attached on the surface of the column. Both the pool and cover gas temperatures have been tracked utilizing thermocouples, and temperature of the inlet gas flow line for the bubble injection is measured with a 0.020-inch thermocouple. The aerosol injection line is heated as well to increase injection bubble temperature up to the sodium pool condition, and a PID control ensures the entire system is in thermal equilibrium. In addition, cover gas pressure has been measured with a SITRANS P410 transmitter with 0-30 psi gauge pressure range. A valve is installed near the top of the sodium pool for sampling, by which the pool condition can be continuously verified. The pool level has also been measured with two-point sensors with $\pm$ 1-inch uncertainty. Particularly, a pressure tank is used to overcome the hydrostatic pressure at the nozzle outlet. The pressure has been kept 1,700 Pa higher than the nozzle exit, and the aerosol generator is placed inside the vessel. Three solenoid valves are used (one for the inlet, and the other two for the outlet) to control the aerosol-dispersed argon gas flow, and the vent outlet maximizes the aerosol concentration inside the bubble. The valves have been controlled with a National Instruments (NI) CRI-9024 Real-Time (RT) Controller, and the cRIO is connected to the data acquisition system. Whole real-time data including temperature, pressure, weight, and flow have been recorded and controlled through NI LabVIEW 2019.

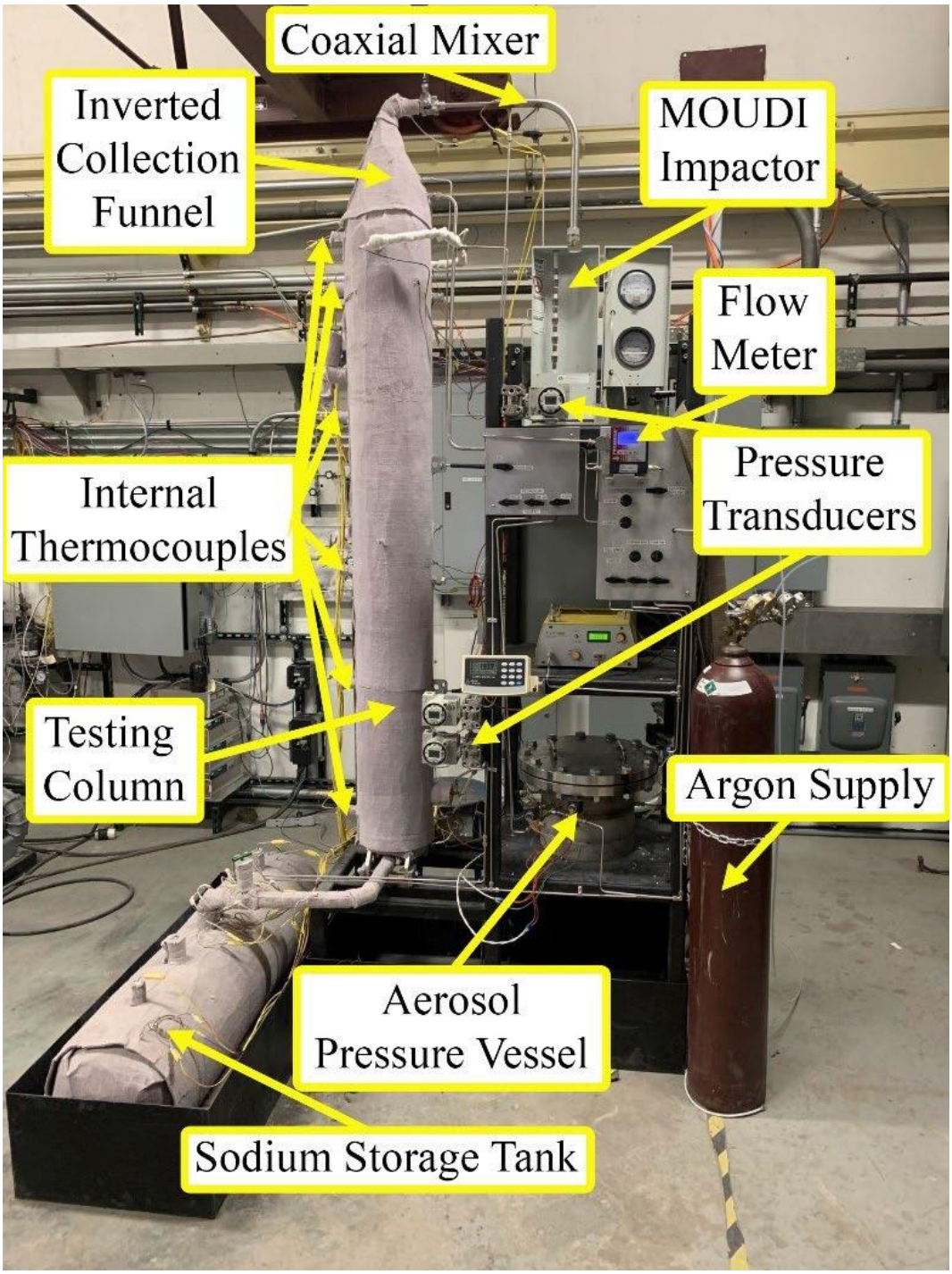

Figure 1. Experimental array for sodium pool scrubbing test [35][1]

[1]This article was published in Nuclear Engineering and Design, Volume 403, K. Becker and M. Anderson, "Experimental validation of simplified radionuclide transport bubble scrubbing code in sodium coolant pool," Article 112137, Copyright Elsevier (2023).

A dilution cross flow, with flow rate of 15 LPM, at 7.5 cm above the sodium free surface enables capturing the escaped aerosols from the sodium pool. Two-sectional gas flows are made for the collector part: 15 LPM at the entrance, and 30 LPM inside a coaxial dilution device at the back-end structure (Figure 2). The coaxial structure is made to meet the target velocity for the particle size measurement. The overall gas flow information has been measured with an Omega FMA6713 flow meter with an uncertainty of 0.3 LPM. Those traveled aerosol particles are captured by an inertial impactor, primarily governed by Stokes number (St) as defined in equation 1.

$$St = \frac{\rho_p C_{slip} V_{nozzle} {d_p}^2}{9\mu_{bulk} D_{nozzle}} \quad (1)$$

Where, ρ_p is particle density, C_{slip} is for slip correction, V_{nozzle} is average velocity at the nozzle exit, d_p is particle diameter, μ_{bulk} is viscosity of the main flow, and D_{nozzle} is nozzle diameter. Dependent upon the Stokes number criterion, particles travel along the mainstream or are trapped through the impaction.

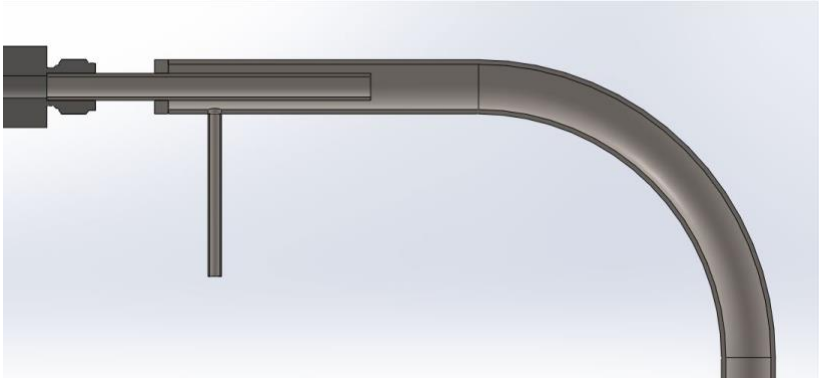

Figure 2. Cross-sectional view of a coaxial dilution line

For the inertial impactor, a MOUDI 10-stage cascade impactor has been used, where 0.056 to 18 um size particles can be collected. There exists a final filter in the impactor, which further enables collecting extensive size range of particulates. Every stage has been rotated to maximize the amount of collection and to achieve uniformity of distribution. Each substrate is coated with aerosolized silicon oil to minimize bounce-back phenomenon of collected particles. After then, those coated specimen have been baked inside furnace at 250 °C for 24 hours to prevent volatility. All weight measurements before and after each test phase have been carried out using CPA26P Sartouruis microbalance with 2 μg scale and $\pm$ 4 μg repeatability.

2.2 Experimental Procedure

Before the pool scrubbing test, the impactor performance has been calibrated by directly connecting the injection nozzle to the MOUDI impactor adopted. Through the process, characteristics of injected aerosols have been quantified. In addition, aerosols lost before the final collection has been assessed considering the trajectory and inverted geometry of the injection nozzle. By the method, loss in the collection system is quantified, and additional loss expected by the downward nozzle has been evaluated by locating the nozzle right below the sodium free surface.

Further, additional source of aerosols by sodium vaporization has been considered. For the purpose, a dilution flow alone above the pool free surface has been made measuring sodium aerosols for each temperature condition, and an additional argon bubble has been injected thereafter to assess the combined effect by bubble burst at the free surface.

To include extensive parametric impacts on the decontamination process and to assess each parameter's sole effect, bubble size, aerosol size/density/concentration, pool height, and system temperature have been considered in the test matrix (TABLE 1). Five repetition tests have been performed for each case to reduce uncertainty and to check the reproducibility of trends. Also, a bubble swarm condition is further considered to reflect multiple bubble effect or bubble breakups. For the purpose, a sparger has been prepared with a linear tube geometry with seven 1.016 mm holes drilled at varying radial positions along the length. Different from single bubble tests, 15 LPM of argon gas is injected for the swarm tests.

TABLE 1. Test matrix considered for sodium pool scrubbing test

Parameter	Unit	Value
Bubble size	cm	2.36 / 2.86 / 3.63 / 4.11 / swarm
Aerosol size	μm	0.018 – 18
Aerosol density	g/cm^3	2.7 (Al) / 8.9 (Ni) / 19.3 (W)
Aerosol concentration	g/m^3	15.3 / 5.4
Pool height	m	1.83 / 0.91
Pool temperature	^{o}C	150 / 200 / 250 / 300

To track bubble dynamics, due to sodium's opaque visibility, radiography is used with a GE Optima XR220 Portable X-Ray and corresponding digital detector (Figures 3 and 4). X-ray images for bubbles are taken with 125 keV and 120 mA power condition, 9 ms exposure period, and 0.6 mm focal size for the X-ray tube. Source-to-object distance has been set to be 101.6 cm, while object-to-image distance is 17.8 cm, which must have sufficient distance considering large dimension of test column and relatively high temperature condition. The X-ray setup has been connected to the LabVIEW system to synchronize with the bubble location. In addition, X-ray images are taken at three locations to derive rise velocities: at the injection nozzle, 80.65 and 117.48 cm above the nozzle inlet.

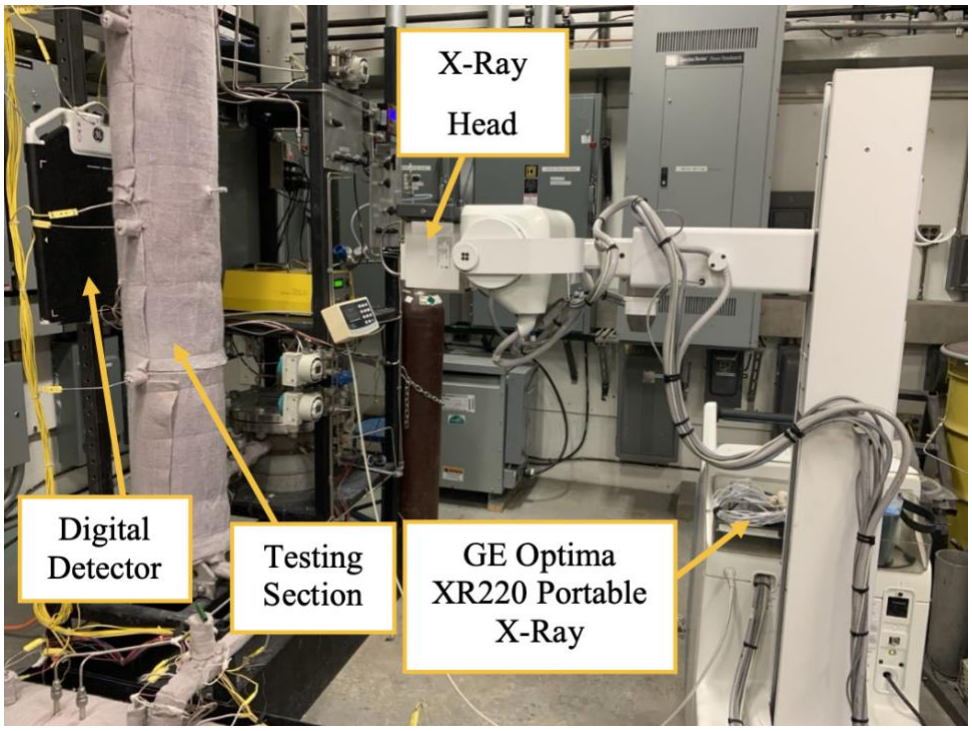

Figure 3. X-ray and digital detector

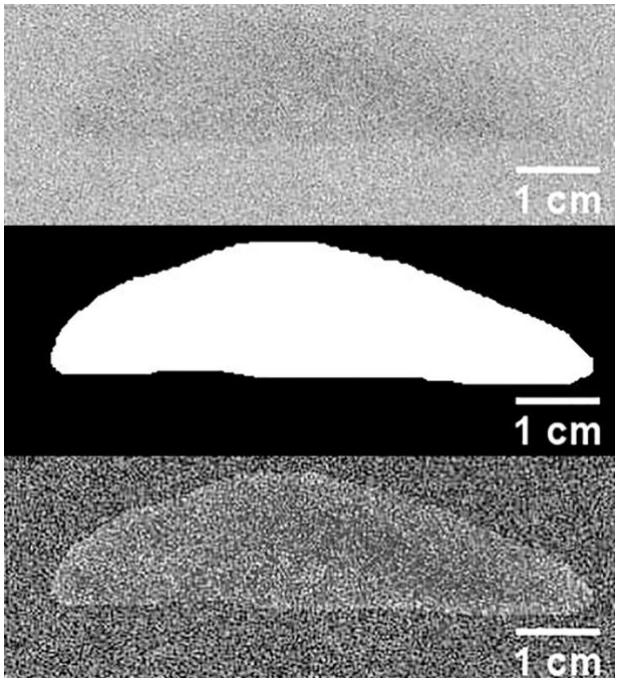

Figure 4. X-ray image for a single bubble: raw, post-processed, and overlay images [35][2]

[2]This article was published in Nuclear Engineering and Design, Volume 403, K. Becker and M. Anderson, "Experimental validation of simplified radionuclide transport bubble scrubbing code in sodium coolant pool," Article 112137, Copyright Elsevier (2023).

For the bubble swarm condition, a surrogate water is used to compensate overlapping phenomenon by multiple bubbles. Using dry air and water as surrogate materials, the bubble characteristics have been visualized with a FASTCAM-Ultima 1024 High-Speed Video Camera, and two backlights (500 W Lowel V-lights). The projected area of bubbles is tracked with ImageJ, and the bubble size in sodium pool with argon gas is calculated back using measured void fraction (Figure 5) based on the ideal gas law. Derived bubble size is larger for the sodium environment compared with water condition, and the process has been validated with single bubbles.

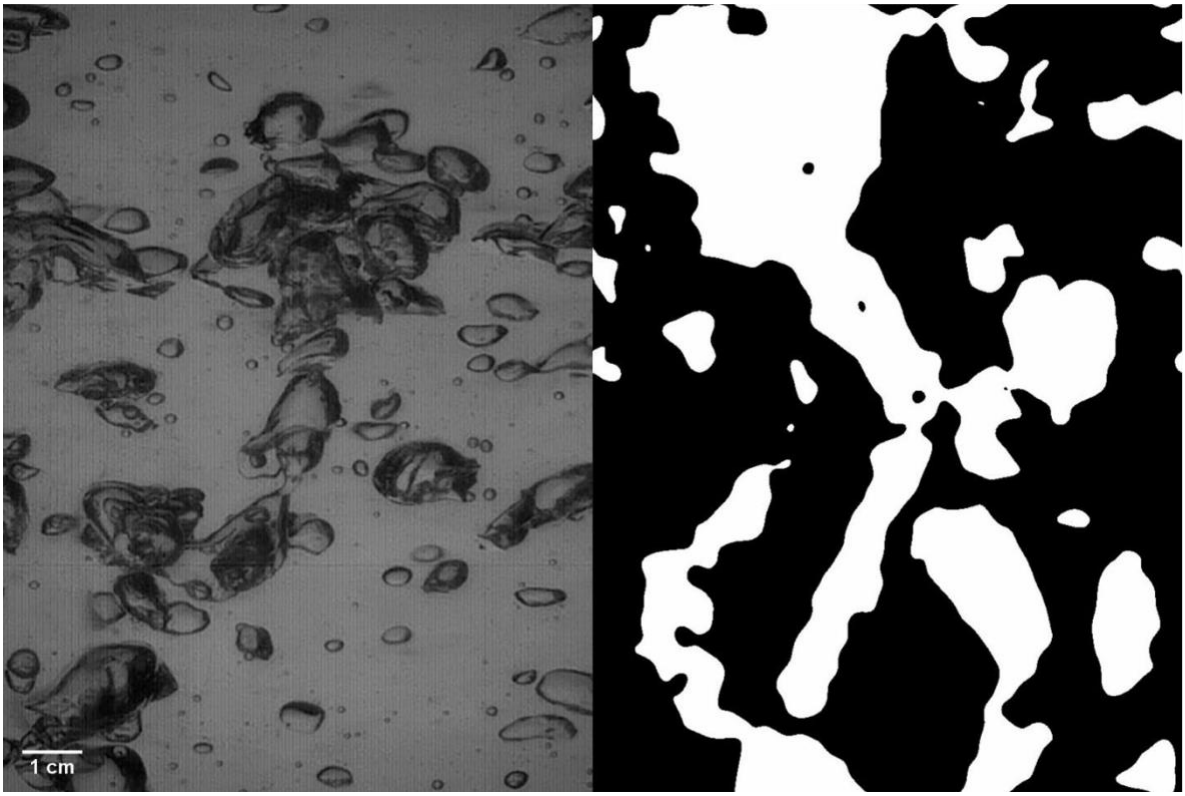

Figure 5. Bubble swarm visualization in water, and projected void area in sodium pool [35][3]

[3]This article was published in Nuclear Engineering and Design, Volume 403, K. Becker and M. Anderson, "Experimental validation of simplified radionuclide transport bubble scrubbing code in sodium coolant pool," Article 112137, Copyright Elsevier (2023).

3 Test Results

3.1 Bubble Size Effect

Four scales of bubble diameters are prepared for the size effect at 200 °C and 1.83 m pool depth with aluminum powders (density of 2.7 g/cm^3) in 15.3 g/m^3 concentration: 2.36 cm, 2.86 cm, 3.63 cm, and 4.11 cm. The considered aerosol size range is from 0.018 μm up to 18 μm. As can be observed in Figure 6, DF tends to be decreased and increased again with aerosol size under the most severe condition (the lowest performance range). At the region, main mechanism changes from Brownian diffusion into inertial impaction and gravitational sedimentation, as the latter phenomena include direct effect of and increasing tendency with particle size. For smaller and larger aerosol size regions, the injected aerosols are expected to be removed inside the pool during bubble rise in almost perfect manner.

With respect to the bubble size effect on DF, the measured DF values are reduced with increasing bubble size since effective interfacial area (expressed in terms of ratio of surface area over volume) decreases, which reduces interaction rate at the surface of bubble during bubble rise. Also, enlarged bubble under single bubble geometry leads to increased rise velocity, which further reduces time periods for pool scrubbing inside sodium pool.

However, the trends are relatively scattered compared with previous water tests [26], where clear differences were observed, as sodium environments accompany much higher uncertainty. Especially in the lowest region, the measured DF results are scattered and sometimes even converged into each other by huge uncertainty, which emphasizes the importance of modeling approaches including uncertainty information in the future.

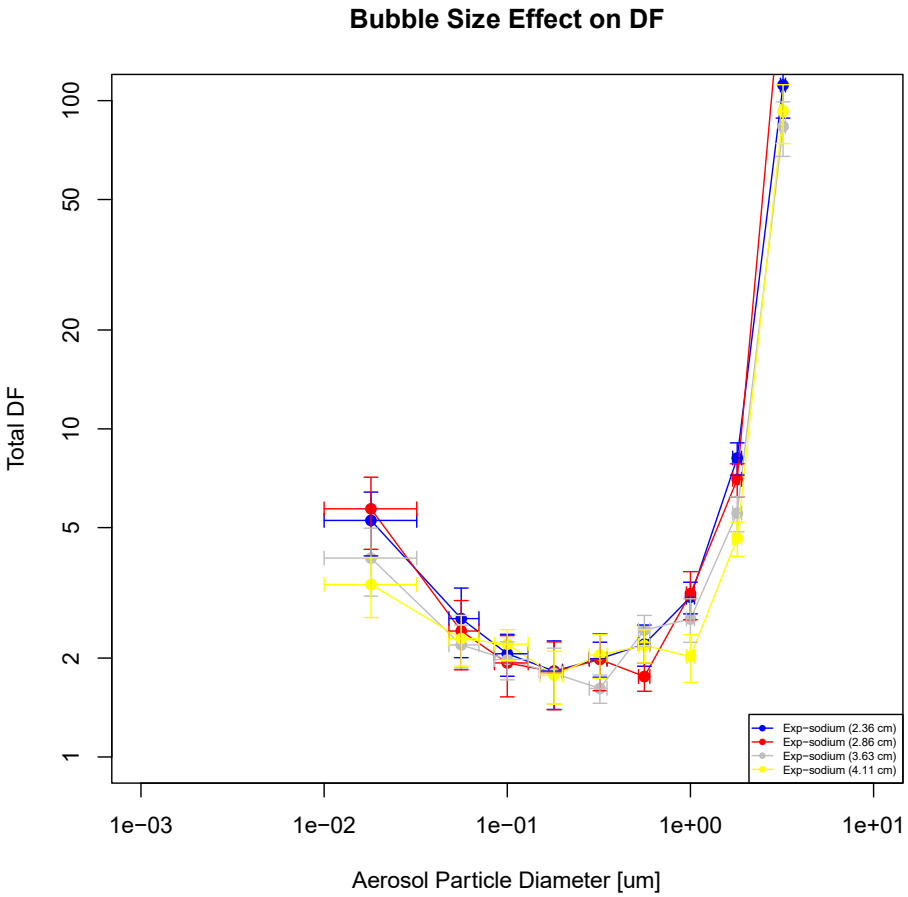

Figure 6. Bubble size effect on DF by measured data

3.2 Aerosol Density Effect

To assess the aerosol density effect, bubble diameter of 3.63 cm at 200 °C and 1.83 m pool depth conditions are prepared with three kinds of powders: aluminum (Al, 2.7 g/cm^3), nickel (Ni, 8.9 g/cm^3), and tungsten (W, 19.3 g/cm^3). All other parameters except the particle density are fixed to derive the density's individual effect on the overall DF performance. Results plotted in Figure 7 show the increasing and decreasing trends with the aerosol size, as observed in previous 'Bubble size effect' section.

In addition, according to the plot, the density effect becomes noticeable at large aerosols, while the effect diminishes and is finally removed at small-sized particles. The trend is related to the consisting mechanisms; both the inertial impaction and gravitational sedimentation that have dominant contribution for large aerosols are strongly affected by particle properties like density, but the Brownian diffusion, a dominant mechanism over small-sized particles, is unaffected by the parameter. For the heaviest material (tungsten in this case), the surging trend at large aerosol region advances, which represents enhanced removal performance, due to emerging and dominant impact of particle properties at the region.

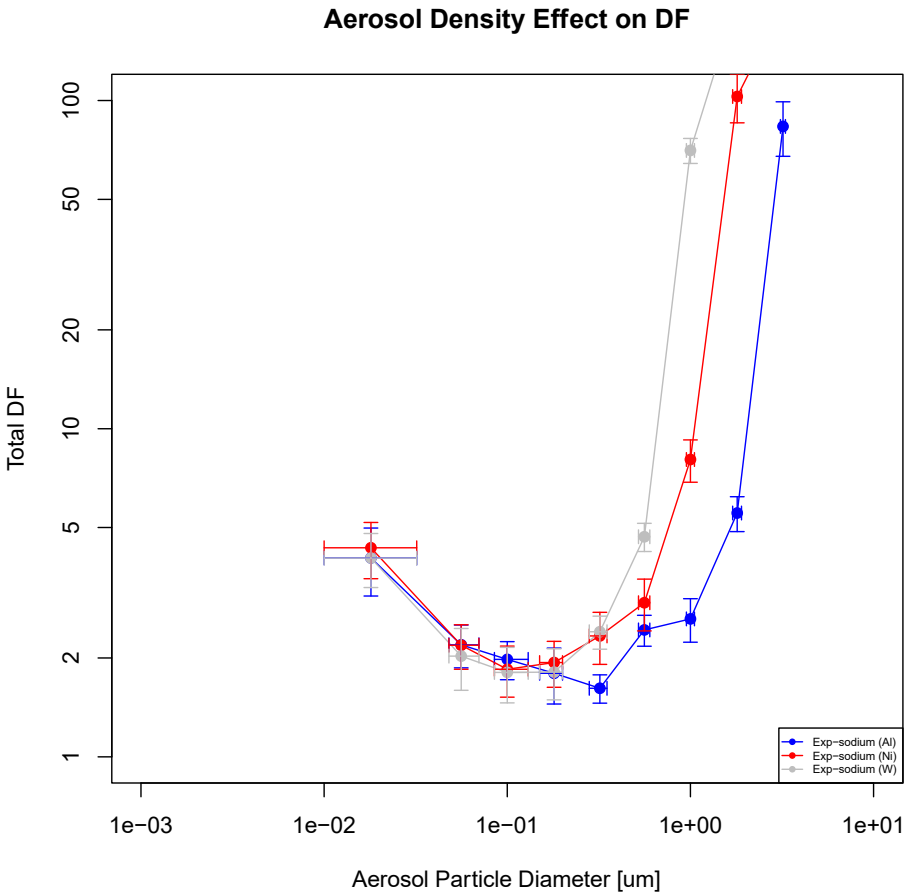

Figure 7. Aerosol density effect on DF

3.3 Aerosol Concentration Effect

Two aerosol concentrations are prepared to evaluate the concentration effect as some previous study has emphasized the importance: 15.3 g/m^3 and 5.4 g/m^3, respectively. The pool condition is kept at 200 ^{o}C with 1.83 m pool height, and aluminum powder has been used as a surrogate aerosol carried inside a 3.63 cm-diameter single bubble.

According to Figure 8, there is almost no effect of concentration within the considered aerosol size region and concentration range. The trend also corresponds with the previous test for water [26], where the high and low concentrations converged with each other for the whole range. The consisting mechanistic models in SRT does not include the parameter as well, which can explain the results. Still, the injected concentration can be used to determine dose impacts toward the environment based on derived DF values and gas volume during integrated simulation, and thus, also plays an important role. Additionally, extreme amount beyond the considered range could add some transient effects, which will also be dependent upon the other parametric conditions.

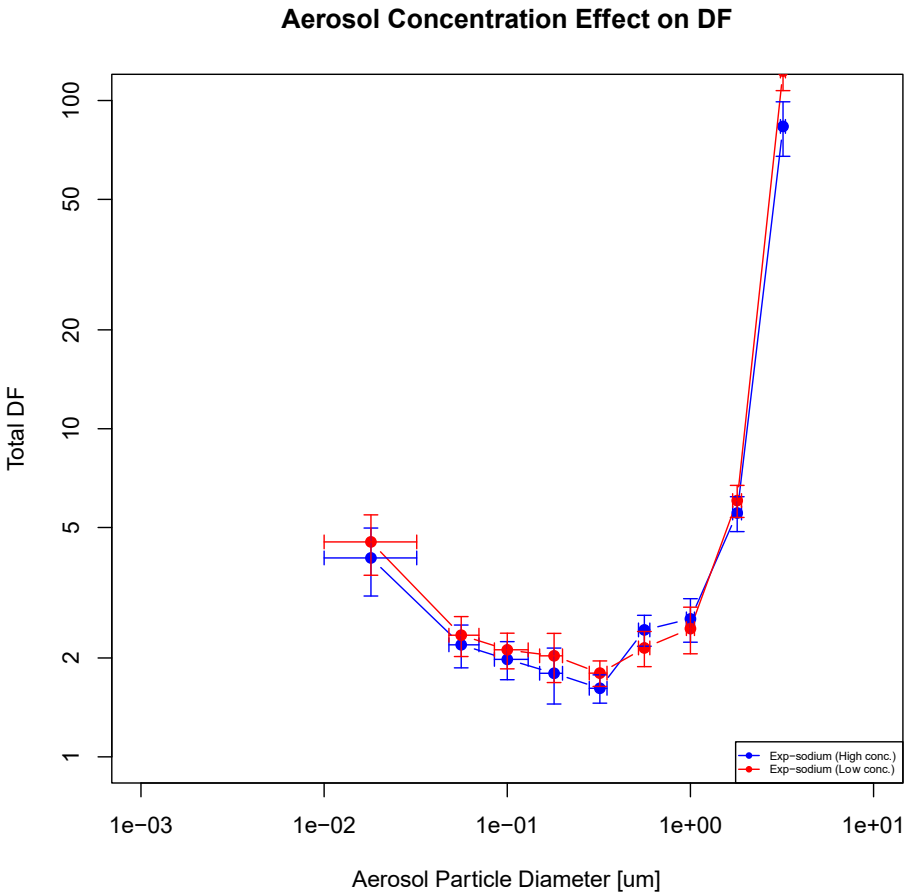

Figure 8. Aerosol concentration effect on DF

3.4 Pool Height Effect

Pool height is related to both local pressure and residence time of bubble rise. Especially, the latter factor determines interaction period inside sodium pool during bubble rise and used for calculating the total amount of reaction through the bubble interface. To address the pool height effect, two levels of sodium pool (1.83 m, and 0.91 m) are prepared at 200 ºC temperature with 3.63 cm bubble diameter. Aluminum particle is adopted to fix the other parameters except the pool height.

As summarized in Figure 9, the pool height effect becomes noticeable at both ends within the considered range, while there exist scatters and even convergences in the middle, as observed in the 'Bubble size effect' section. Again, due to relatively increased uncertainty under sodium condition in the range, such ambiguous tendency has been observed. However, the plots keep the expected trends and correspond with the previous water test overall [26], and the scatter can be treated to be minor considering the scale of plot. Based on the overall trends, pool depth plays an important role, and the parametric effect greatly increases at small- or large-sized aerosols, also observed through the water test.

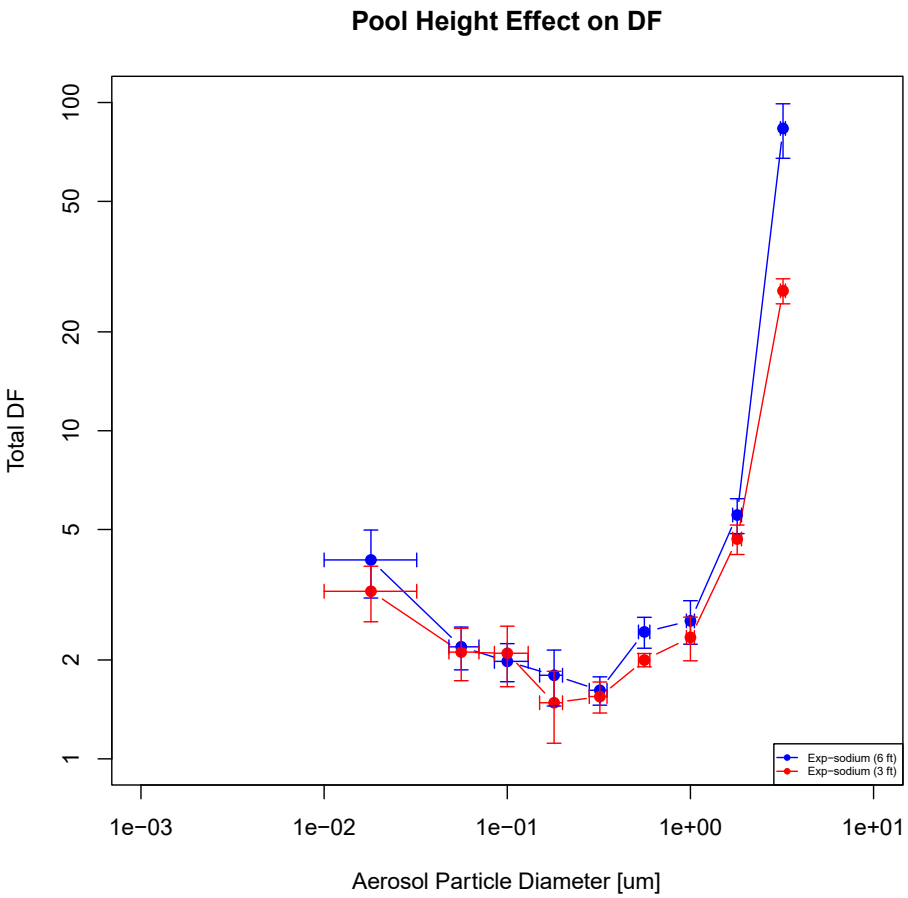

Figure 9. Pool height effect on DF

3.5 System Temperature Effect

Sodium coolant accompanies relatively high temperature environments compared with a water condition, which is expected to provide effect on consisting mechanisms and to induce increased degree of vaporization. In this regard, four temperature conditions have been considered (150 ºC, 200 ºC, 250 ºC, and 300 ºC) at 1.83 pool height condition with aluminum aerosols. Due to the sensitiveness of bubble volume with temperature, the measured effective bubble diameter varies for each temperature condition: 3.28 cm (150 ºC), 3.63 cm (200 ºC), 3.86 cm (250 ºC), and 4.12 cm (300 ºC).

The plotted trends in Figure 10 follow the previous plots, where measured DF values decrease and increase with increasing aerosol size, as the major mechanism changes. However, the effect of system temperature below 300 ºC is relatively minor for the range of interest. The temperature gap within the considered range provides marginal effect to the included mechanisms and to the vaporized sodium-induced capture.

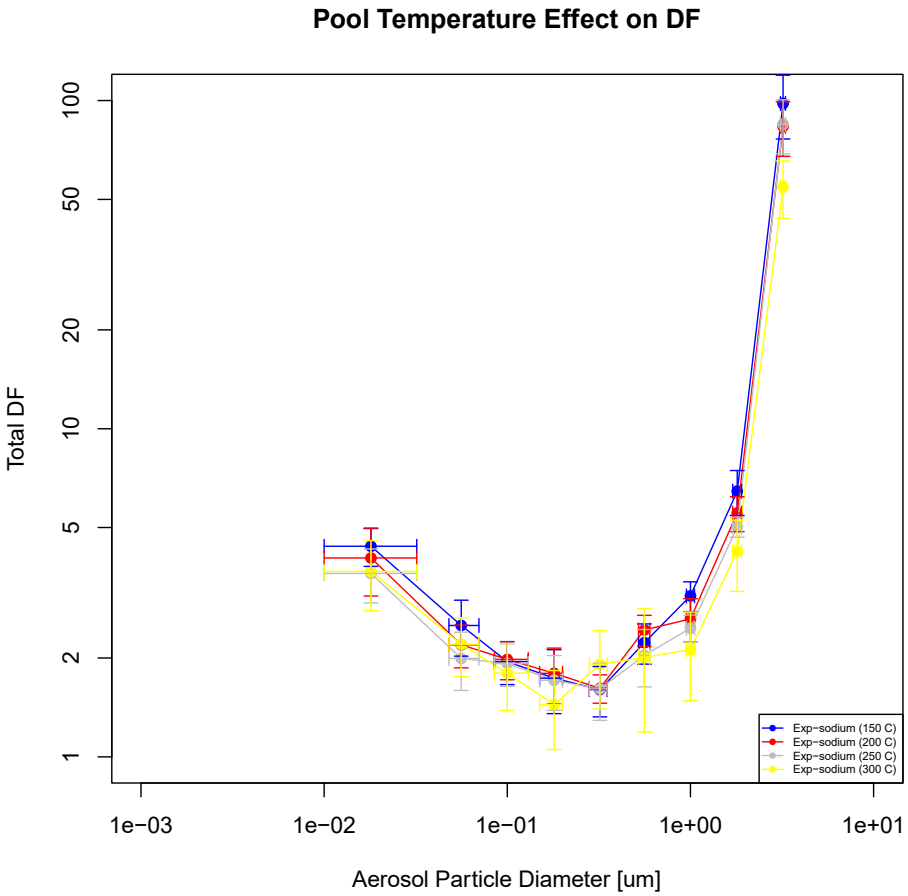

Figure 10. System temperature effect on DF

3.6 Bubble Swarm Effect

To reflect bubble breakups or multiple bubble generation during fuel pin failure, bubble swarm condition has been further considered in this section. For the purpose, heterogeneous bubbles are made using a sparger at 200 °C, and 1.83 m pool height with aluminum powders. Based on the radiography of bubbles inside sodium pool and relationship made from the surrogate water condition, an average void fraction has been found to be 0.379, and the corresponding volume-weighted mean bubble diameter is 3.66 cm.

The swarm effect has been compared with a single bubble condition of similar bubble size (3.63 cm) in Figure 11. According to the figure, the overall trend follows the previous parametric effects, but the minimum DF value is increased under the bubble swarm regime. The enhancement may attribute to active bubble interaction such as coalescence and additional breakups, or turbulence during bubble rise.

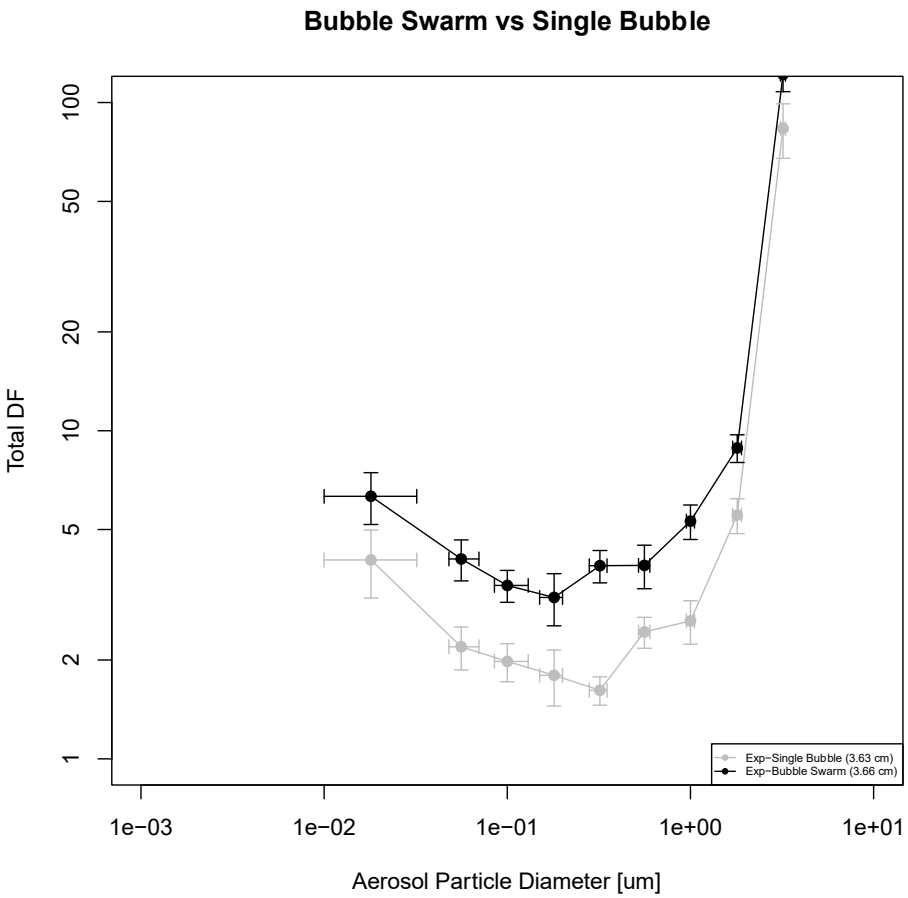

Figure 11. Bubble swarm effect against a single bubble condition

4 Conclusion

Pool scrubbing tests in a sodium pool have been carried out by the University of Wisconsin-Madison [35], with consideration of independent effects by each major parameter: bubble size, aerosol size, aerosol density, aerosol concentration, pool depth, system temperature, and bubble swarm condition. The target parameters have been selected based on the SRT code made for MST analysis in advanced reactors. Additionally, target range has been determined from the SRT prediction, where the lowest performance of decontamination is expected, which will lead to the dominant radionuclide escape from the sodium pool. The measured data have been assessed in terms of trends and parametric effects.

According to the overall trends, the decontamination performance decreases and increases again with aerosol size, with the change of major removal mechanism from Brownian diffusion into inertial impaction and gravitational sedimentation. Both the measured and predicted data show the lowest performance within the considered range, and DF values radically expands at both ends.

For the bubble size effect, four dimensions of bubbles have been considered by controlling the valve opening periods. DF tends to increase with decreasing bubble size since interfacial area over unit volume increases. In addition, for a single bubble, bubble rise velocity decreases with decreasing bubble size as well, which affects bubble residence periods inside the sodium pool. When the aerosol density effect is concerned, the effect becomes noticeable for large aerosols, while it diminishes and is finally removed for small-sized aerosols. The trend is related to the change of removal mechanism; both inertial impaction and gravitational sedimentation include the density effect in an increasing manner with the particle size, while Brownian diffusion is irrelevant to the material density. Also, as the experiment has extended the considered density condition up to heavier material (tungsten), even the heavy elements of released radionuclides such as actinides, expected to be released during the fuel pin failure, could now be covered. In contrast, an aerosol concentration effect is negligible in the range of interest, also observed through the previous water tests. Concentration is not included in any of describing mechanisms for the pool scrubbing process. With respect to the pool height effect, more aerosols are removed at deeper condition since bubble residence period elongates. However, difference between two pool height minimizes at the lowest performance range, which sometimes induces convergence between two conditions by data scatter. In addition, a pool temperature effect has been addressed, and the effect is relatively marginal below 300 ^{o}C, compared with other parametric effects (except the aerosol concentration). Even though consisting mechanisms are affected by temperature, the impact turned out to be minor compared with other parameters under the considered range. As an additional approach, a bubble swarm condition has been further included to assess the multiple bubble effect. The swarm condition, a realistic condition during accidents, has induced increased DF performance against the single bubble tests, possibly made through bubble interactions or turbulence around the herd. Here again, the overall trend of DF values follows the single bubble experiments, but with increased removal performance.

As a future work, extensive simulations will be proceeded as done for the water condition, reflecting each parameter's inherent uncertainty information. Specifically, DF by the mean values of each parameter (nominal case) and DF spans by uncertainties will be considered. The approach

is expected to provide meaningful results especially for regions with huge uncertainty, where measurement values are highly scattered.

REFERENCE

[1] U.S. Nuclear Regulatory Commission, "Accident source terms and siting for small modular reactors and non-light water reactors," SECY-16-0012, 2016.

[2] U.S. Nuclear Regulatory Commission, "Guidance for a technology-inclusive, risk-informed, and performance-based methodology to inform the licensing basis and content of applications for licenses, certifications, and approvals for non-light water reactors," Regulatory Guide 1.233 Revision 0, 2020.

[3] D. Grabaskas, M. Bucknor, J. Jerden, A. Brunett, M. Denman, A. Clark, and R. Denning, "Regulatory technology development plan - sodium fast reactor: mechanistic source term development – trial calculation," Argonne National Laboratory, ANL-ART-49, 2016.

[4] N. Fuchs, "The mechanics of aerosols," Oxford: Pergamon Press, 1964.

[5] A. Wassel, A. Mills, and D. Bugby, "Analysis of radionuclide retention in water pools," Nucl. Eng. Des., 90(1), pp. 87-104, 1985.

[6] P. Owczarski and K. Burk, "SPARC-90: A code for calculating fission product capture in suppression pools," Pacific Northwest Laboratory, NUREG/CR-5765, 1991.

[7] D. Powers and J. Sprung, "A simplified model of aerosol scrubbing by a water pool overlying core debris interacting with concrete," Sandia National Laboratories, NUREG/CR-5901, 1993.

[8] S. Ramsdale, S. Guentay, and H. Friederichs, "BUSCA-JUN91 reference manual," Paul Scherrer Institut, ISSN 1019-0643, 1995.

[9] T. Kanai, M. Furuya, T. Arai, and Y. Nishi, "Development of an aerosol decontamination factor evaluation method using an aerosol spectrometer," Nucl. Eng. Des., 303, pp. 58-67, 2016.

[10] M. Bucknor, M. Farmer, and D. Grabaskas, "An assessment of fission product scrubbing in sodium pools following a core damage event in a sodium cooled fast reactor," International Conference on Fast Reactors and Related Fuel Cycles: Next Generation Nuclear Systems for Sustainable Development (FR 17), Yekaterinburg, Russia, 2017.

[11] Y. Kim, D. Kam, J. Yoon, and Y. Jeong, "The importance of representative aerosol diameter and bubble size distribution in pool scrubbing," Ann. Nucl. Energy, 147, Article 107712, 2020.

[12] Y. Lee, Y. Cho, and I. Ryu, "Preliminary analyses on decontamination factors during pool scrubbing with bubble size distributions obtained from EPRI experiments," Nucl. Eng. Technol., 53(2), pp. 509-521, 2021.

[13] D. Kam, D. Grabaskas, K. Becker, M. Anderson, T. Starkus, and M. Bucknor, "Using calibrated water data for preliminary validation of the SRT code for advanced reactors," Topical Issues in Nuclear Installation Safety, Vienna, Austria, 2022.

[14] I. Kaneko, M. Fukasawa, M. Naito, K. Miyata, and M. Matsumoto, "Experimental study on aerosol removal effect by pool scrubbing," 22nd DOE/NRC Nuclear Air Cleaning and Treatment Conference, Denver, United States, 1992.

[15] M. Marcos-Crespo, F. Gomez-Moreno, I. Melches-Serrano, M. Martin-Espigares, and J Lopez-Jimenez, "LACE-Espana experimental programme on the retention of aerosols in water pools," CIEMAT, CIEMAT-740, 1994.

[16] M. Swiderska-kowalczyk, M. Escudero-Berzal, M. Marcos-Crespo, M. Martin-Espigares, and J. Lopez-Jimenez, "State-of-the-art review on fission product aerosol pool scrubbing under severe accident conditions," CIEMAT, INIS-PL-0001, 1995.

[17] L. Herranz, M. Escudero, V. Peyres, J. Polo, and J. Lopez-Jimenez, "Review and assessment of pool scrubbing models," CIEMAT, CIEMAT-784, 1996.

[18] A. Dehbi, D. Suckow, and S. Guentay, "Aerosol retention in low-subcooling pools under realistic accident conditions," Nucl. Eng. Des., 203(2-3), pp. 229-241, 2001.

[19] A. Dehbi, D. Suckow, T. Lind, S. Gueentay, S. Danner, and R. Mukin, "Key findings from the artist project on aerosol retention in a dry steam generator," Nucl. Eng. Technol., 48(4), pp. 870-880, 2016.

[20] J. Lee, W. Jung, H. Lee, G. Kim, and D. Lee, "Experimental study on aerosol scrubbing efficiency of self-priming venturi scrubber submerged in water pool," Ann. Nucl. Energy, 114, pp. 571-585, 2018.

[21] S. Kim, J. Lee, J. Jung, K. Ha, H. Kim, and J. Song, "Introduction of filtered containment venting system experimental facility in KAERI and results of aerosol test," Nucl. Eng. Des., 326, pp. 344-353, 2018.

[22] Y. Li, Z. Sun, H. Gu, and Y. Zhou, "Deposition characteristic of micro-nano soluble aerosol under bubble scrubbing condition," Ann. Nucl. Energy, 133, pp. 881-888, 2019.

[23] H. Diao, Y. Zhou, H. Gu, Y. Li, and C. Yan, "Experimental study on the scrubbing efficiency of aerosols contained in horizontal and vertically downward submerged gas jet," Prog. Nucl. Energ., 126, Article 103406, 2020.

[24] Y. Choi, D. Kam, P. Papadopoulos, T. Lind, and Y.H. Jeong, "Experimental investigation on bubble behaviors in a water pool using the venturi scrubbing nozzle," Nucl. Eng. Technol., 53(6), pp. 1756-1768, 2021.

[25] Y. Kim, J. Yoon, and Y. Jeong, "Experimental study of the nozzle size effect on aerosol removal by pool scrubbing," Nucl. Eng. Des., 385, 15, Article 111544, 2021.

[26] K. Becker and M. Anderson, "Experimental study of SRT scrubbing model in water coolant pool," Nucl. Eng. Des., 377, Article 111130, 2021.

[27] W. Jung, D. Lee, J. Kang, M. Ko, B. Kim, J. Lee, D. Lee, B. Lee, and K. Ha, "Experimental study of pool scrubbing under horizontal gas injection," Ann. Nucl. Energy, 171, Article 109014, 2022.

[28] B. Lee, S. Kim, and K. Ha, "Separate and integral effect tests of aerosol retention in steam generator during tube rupture accident," Nucl. Eng. Technol., 54(7), pp. 2702-2713, 2022.

[29] S. Kim, C. Kang, J. Kim, K. Park, J. Oh, B. Lee, K. Ha, and S. Hong, "Evaluation of aerosol retention inside a steam generator under steam generator tube rupture accident conditions," Nucl. Eng. Des., 396, Article 111899, 2022.

[30] J. Yoon, Y. Kim, and Y. Jeong, "Observation of the jet transition at a single vertical nozzle under pool scrubbing conditions," Ann. Nucl. Energy, 171, Article 109041, 2022.

[31] S. Miyahara, N. Sagawa, and K. Shimoyama, "Iodine mass transfer from xenon-iodine mixed gas bubble to liquid sodium pool, (I) Experiment," J. Nucl. Sci. Technol., 33(2), pp. 128-133, 1996.

[32] S. Miyahara and N. Sagawa, "Iodine mass transfer from xenon-iodine mixed gas bubble to liquid sodium pool, (II) Development of analytical model," J. Nucl. Sci. Technol., 33(3), pp. 220-228, 1996.

[33] D. Kam, D. Grabaskas, T. Starkus, M. Bucknor, and A. Uchibori, "A preliminary validation study for removal performance of iodine gas in sodium pool with a simplified approach," ANS Annual Meeting, California, United States, June 12-16, 2022.

[34] A. Pradeep and A. Sharma, "Semiempirical model for wet scrubbing of bubble rising in liquid pool of sodium-cooled fast reactor," Nucl. Eng. Technol., 50, pp. 849-853, 2018.

[35] K. Becker and M. Anderson, "Experimental validation of simplified radionuclide transport bubble scrubbing code in sodium coolant pool," Nucl. Eng. Des., 403, Article 112137, 2023.

APPENDIX

- Parametric uncertainty table

Bubble diameter		**Pool depth**		**Pool temperature**	
Mean[cm]	Uncertainty[%]	Mean[m]	Uncertainty[%]	Mean[°C]	Uncertainty[%]
2.36	4.87	1.83	1.39	150	1.47
2.86	4.85	0.91	2.78	200	1.10
3.63	6.08			250	0.88
4.11	8.26		-	300	0.73
3.66 (swarm)	13.16				-

- Aerosol size uncertainty table

Aerosol particle size		
Mean [μm]	Minus	Plus
18	6	4
10	1.25	0.5
5.6	0.6	0.4
3.2	0.1	0.1
1.8	0.1	0.1
1	0.05	0.05
0.56	0.04	0.04
0.32	0.04	0.03
0.18	0.03	0.02
0.1	0.015	0.03
0.056	0.008	0.014
0.018	0.008	0.014

Nuclear Science and Engineering
Argonne National Laboratory
9700 South Cass Avenue, Bldg. 208
Argonne, IL 60439

www.anl.gov

Argonne National Laboratory is a U.S. Department of Energy laboratory managed by UChicago Argonne, LLC